

See discussions, stats, and author profiles for this publication at: <https://www.researchgate.net/publication/231647576>

Sonoluminescence of Tb(III) at the Extended Solid–Liquid Interface

ARTICLE in THE JOURNAL OF PHYSICAL CHEMISTRY C · MAY 2011

Impact Factor: 4.77 · DOI: 10.1021/jp202045b

CITATIONS

3

READS

24

4 AUTHORS:



Matthieu Viot

Institut de Chimie Séparative de Marcoule

19 PUBLICATIONS 273 CITATIONS

SEE PROFILE



Rachel Pflieger

Institut de Chimie Séparative de Marcoule

32 PUBLICATIONS 188 CITATIONS

SEE PROFILE



Johann Ravaux

Institut de Chimie Séparative de Marcoule

46 PUBLICATIONS 288 CITATIONS

SEE PROFILE



Sergey Nikitenko

Atomic Energy and Alternative Energies Com...

79 PUBLICATIONS 1,225 CITATIONS

SEE PROFILE

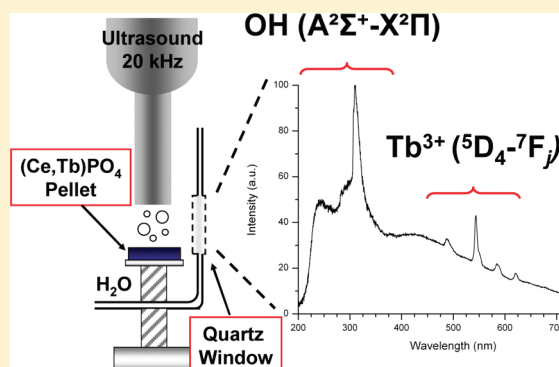
Sonoluminescence of Tb(III) at the Extended Solid–Liquid Interface

Matthieu Viro, Rachel Pflieger, Johann Ravau, and Sergey I. Nikitenko*

Institut de Chimie Séparative de Marcoule (ICSM), UMR 5257 ICSM Site de Marcoule, BP 17171, 30207 Bagnols sur Cèze, France

Supporting Information

ABSTRACT: For the first time, acoustic cavitation was used as a source of excitation for photoactive species contained in an extended solid phase. Spectroscopic measurements performed during the sonication of $(\text{Ce}_{0.9}\text{Tb}_{0.1})\text{PO}_4$ sintered pellets with 20 kHz power ultrasound in cooled water under argon showed the Tb(III) light emission resulting from $^5\text{D}_4\text{--}^7\text{F}_j$ f–f transitions. The emission spectra were measured as a function of the focus within the cavitation zone, as a function of the distance between the pellet and the ultrasonic horn, or using sonoluminescence quenchers (air or *tert*-butanol). The experiments revealed that Tb(III) sonoluminescence results from a solid-state Tb(III) excitation by photons emitted from the cloud of ultrasonically driven cavitation bubbles, referred to as “sonophotoluminescence”.



1. INTRODUCTION

The propagation of an acoustic wave in a liquid medium may lead to the formation, growth, and violent collapse of vapor filled microbubbles.^{1,2} This phenomenon, called acoustic cavitation, is known to be responsible for the production of extreme transient conditions within the collapsing bubbles (“hot spots”), resulting in chemical reactions (sonochemistry)^{3,4} and emission of light in the UV–vis optical range (sonoluminescence, SL).^{1,4–8} Only a few studies have examined SL as a source of excitation for photoactive species contained in the treated media. Recently, Ashokkumar and Grieser reported the *in situ* excitation of pyranine with 515 kHz power ultrasound in aqueous solution.⁹ The observed emission spectrum of pyranine was shown to be triggered by multibubble SL and not by chemical reactions that could occur between solutes and radicals produced within the bubbles.¹⁰ The highlighted phenomenon, referred to as “sonophotoluminescence”,^{9,11} was then observed for other organic fluorescent species in aqueous and nonaqueous solutions.^{12,13} Later, low-resolution sonoluminescence spectra of lanthanide ions were reported for concentrated aqueous solutions of lanthanide salts submitted to 20 kHz power ultrasound.^{14,15} It was suggested that the SL of Ln(III) in solutions is governed by two major processes: (i) sonophotoluminescence and (ii) collisional excitation of Ln(III) ions with the “hot” particles (radicals, excited molecules, etc.) at the bubble/solution interface. Recently, the reported light emission observed during sonication of organic^{16–18} and inorganic¹⁹ solid powders in appropriate solvents was shown to originate rather from triboluminescence than from “true” sonoluminescence.

In view of the above, ultrasound-induced excitation of lanthanides appears to be a quite new topic that remains poorly documented. Furthermore, most of the reported studies are related to homogeneous systems, and the investigations dealing with solid–liquid interfaces are even scarcer. To the best of our

knowledge, SL-induced excitation of photoactive species has never been studied close to an extended solid boundary. Herein, we report the excitation of Tb(III) under acoustic cavitation at the vicinity of a synthesized lanthanide phosphate pellet: $(\text{Ce}_{0.9}\text{Tb}_{0.1})\text{PO}_4$. Because of their very interesting properties (high quantum yield of luminescence, very low solubility in water, high melting points, chemical and thermal stability), lanthanide phosphates constitute promising matrices for several applications such as biological imaging, light phosphor powders, plasma display panels, LEDs, cathode ray tubes, etc.^{20–22}

2. EXPERIMENTAL METHODS

In typical experiments, a thermostated cylindrical reactor is mounted on top of a manufactured Teflon sample holder allowing holding tightly the solid sample as shown in Figure 1. The sample holder comprises a screw which permits to sonicate the solid sample at reproducible and controlled distance from the ultrasonic probe (1 cm², 20 kHz, 750 W). The ultrasonic titanium horn (Vibra-cell, Sonics & Materials) is mounted on top of the reactor (opposite the sample holder) and fixed with a Teflon ring allowing its reproducible immersion in deionized water (250 mL). A new horn tip is used for each experiment to avoid the drop of SL due to the tip cavitation erosion. Experiments are conducted at 20 kHz under argon flow. Argon is bubbled ($\sim 100 \text{ mL min}^{-1}$) through the water 30 min before sonication and during the whole experiments. The acoustic power (P_{ac}) and ultrasonic intensity (I_{ac}) delivered to the solution are determined using the conventional thermal probe method.^{23,24} The steady-state temperature of $9 \pm 1 \text{ }^\circ\text{C}$ inside the reactor is controlled during the entire ultrasonic treatment with a Lauda

Received: March 3, 2011

Revised: April 19, 2011

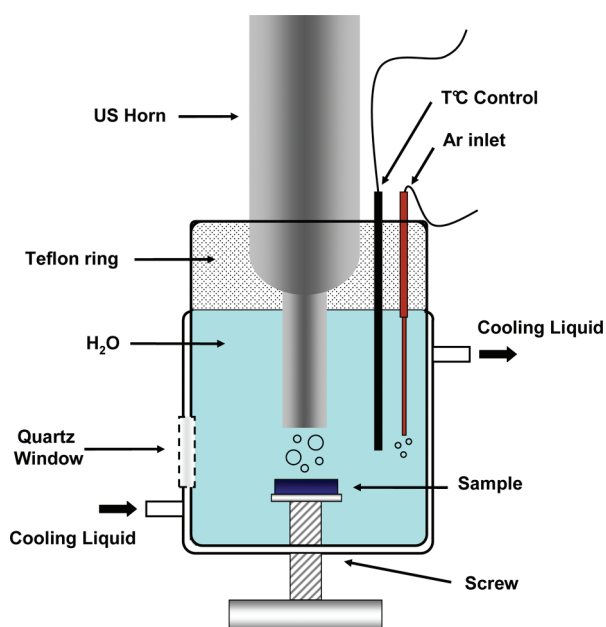


Figure 1. Simplified representation of the experimental setup.

RE 210 cryostat and measured by means of a thermocouple inserted in the cell. The experiments are performed in deionized Milli-Q water (250 mL, resistivity higher than $18.2 \text{ M}\Omega \cdot \text{cm}$ at 25°C).

Light emitted from the cell is collected through a quartz window and imaged onto the 0.1 mm slit of the spectrometer (SP 2356i, Roper Scientific; gratings 300 gr/mm blz 300 and 150 gr/mm blz 500) coupled to a CCD camera (Spec10-100BR with UV coating, Roper Scientific) cooled with liquid nitrogen. Sonoluminescence spectra are recorded from 250 to 700 nm (with appropriate filters to avoid second-order light emission). Spectral calibration is done with a Hg(Ar) Pen-Ray lamp (LSP035, LOT-Oriel). Presented spectra are the averages of at least two spectra acquired during 300 s each and corrected for background noise and quantum efficiencies of gratings and CCD.⁸ The experiments were performed with the pellets obtained after compaction and sintering of the $(\text{Ce}_{0.9}\text{Tb}_{0.1})\text{PO}_4 \cdot n\text{H}_2\text{O}$ powder precipitated from aqueous solutions, which crystallized in the hexagonal rhabdophane-type phase identified against JCPDS file No. 034-1380 (see Supporting Information).^{21,22} In agreement with the literature, the monoclinic monazite phase was observed for the sintered phosphates (JCPDS file No. 032-0199; see the comparison of the patterns in Figure S1, Supporting Information).²⁰ The lanthanide/phosphate ratio of the pellets was checked by using energy dispersive X-ray spectroscopy (EDX) and was found to be about 1:1, which was in agreement with what added in the synthesis step. Further characterization of the precipitated powder and the sintered pellets was finally done with scanning electron microscopy (SEM; see Figure S2, Supporting Information).

3. RESULTS AND DISCUSSION

The sonication of $(\text{Ce}_{0.9}\text{Tb}_{0.1})\text{PO}_4$ pellet with optimized settings allowed the observation of a luminescence spectrum ranging from 250 to 700 nm, constituted by a continuum superimposed with particular features (Figure 2). The broad continuum can be attributed to bremsstrahlung, to $\text{H} + \text{OH}^\bullet$ recombination, and possibly to water molecules deexcitation or $\text{OH}(\text{B}^2\Sigma^+ - \text{A}^2\Sigma^+)$ emission.⁸ The intense emission extending

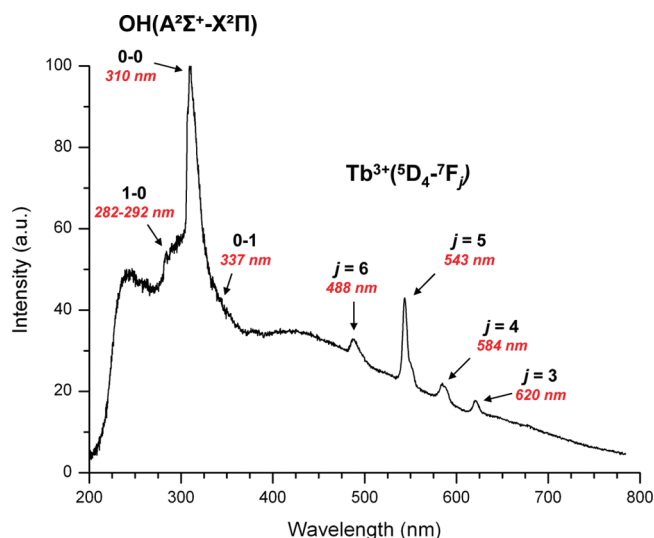


Figure 2. SL spectrum obtained for the sonication of $(\text{Ce}_{0.9}\text{Tb}_{0.1})\text{PO}_4$ pellet with optimized settings (short horn–sample distance, focusing near the ultrasonic horn, $9 \pm 1^\circ \text{C}$, Ar, $I: \sim 18 \text{ W cm}^{-2}$).

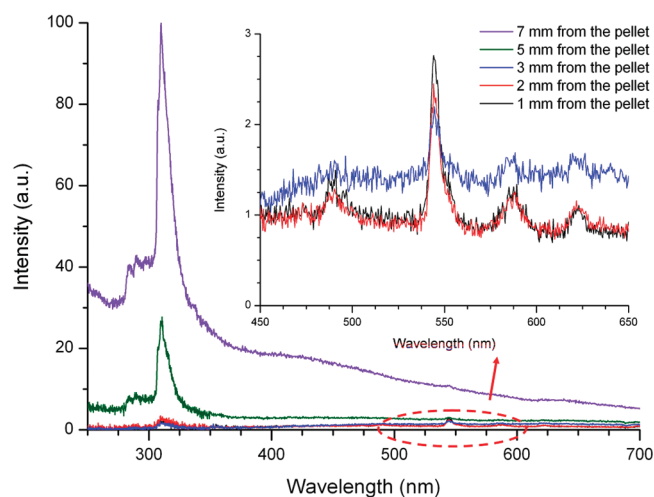


Figure 3. Evolution of the SL spectra measured from close to the sample surface (~ 1 mm, black curve) to far from it (~ 7 mm, purple curve). The horn–pellet distance is kept at ~ 1 cm ($9 \pm 1^\circ \text{C}$, Ar, $I: \sim 18 \text{ W cm}^{-2}$). The values indicated in the caption indicate a stepwise evolution of the focus within the cavitation cloud. Insert: zoom of the 450–650 nm range.

from 270 to 350 nm arises from $\text{OH}(\text{A}^2\Sigma - \text{X}^2\Pi)$ transitions. The dominant peak at 310 nm corresponds to the 0–0 transition, followed by the 1–0 transition between 282 and 292 nm, and a small shoulder around 340 nm (0–1 transition).⁸ The most striking feature stands out in the visible range where four emission peaks are displayed at 488, 543, 584, and 620 nm. These transitions are not observed during pure water sonication and can be attributed to Tb(III) f–f transitions between $^5\text{D}_4$ excited state and $^7\text{F}_j$ ground states, or to the $^5\text{D}_4 - ^7\text{F}_6$, $^5\text{D}_4 - ^7\text{F}_5$, $^5\text{D}_4 - ^7\text{F}_4$, and $^5\text{D}_4 - ^7\text{F}_3$ transitions, respectively. This was found to be in agreement with the literature dealing with photoluminescence excitation of Tb(III)-doped Ce(III) orthophosphates.^{20–22} Note that $^5\text{D}_3 - ^7\text{F}_j$ blue transitions are not observed in our spectra probably due to their emission quenching by the cross relaxation

effect, resulting in an intense and characteristic Tb(III) green emission at ~ 543 nm.²⁵ In principle, an energy transfer from Ce(III) to Tb(III) could also affect the intensity of 5D_4 emissions; however, the relatively weak Ce(III) emission, consisting in a broad peak around ~ 310 – 410 nm centered at ~ 355 nm, is not observed in our experiments.^{15,20,25}

To investigate the mechanism of Tb(III) ultrasonic excitation, we fixed the distance between the ultrasonic horn and the $(\text{Ce}_{0.9}\text{Tb}_{0.1})\text{PO}_4$ sample at ~ 1 cm, and we collected the emission spectra stepwise along the z axis, from the sample surface toward the ultrasonic horn. This approach permits to follow the simultaneous evolution of Tb(III) and OH^* emission lines as a function of the focus position within the cavitation cloud. These spectra are shown in Figure 3. As expected, $\text{OH}(A^2\Sigma^+ - X^2\Pi)$ transitions are very intense when focusing close to the ultrasonic horn. On the contrary, they are very weak far from it, i.e., at the vicinity of the pellet surface. In the visible range, we note the presence of Tb(III) emission lines in the spectra collected near the sample. The intensity of the main transition ($^5D_4 - ^7F_5$) within the cavitation cloud may then be considered (inset of Figure 3). As shown, this peak exhibits a maximum intensity at the vicinity of the sample surface and then decreases rapidly as a function of the distance from the pellet. In the same way, the intensity of the other Tb(III) lines decreases with the distance until they disappear.

The SL spectra evolution demonstrated in Figure 3 supports the idea that Tb(III) emission is resulting from a solid phase excitation, and not from an excitation of dissolved Tb(III) ionic species or dispersed solid particles of monazite contained in the liquid phase. Moreover, the negligible light absorption in the range of 250 – 300 nm confirms the absence of Tb(III) species in solution. Indeed, lanthanide phosphates are known for their scarcely low solubility in water ($K_s \sim 10^{-27}$ – 10^{-24} at 25 °C).^{26,27} The absence of Ce and Tb in solution was confirmed using ICP-AES analysis after 8 h of sonication at ~ 1 cm distance from the sonotrode although Tb(III) light emission was observed during that time. On the other hand, triboluminescence cannot be considered as a reasonable excitation mechanism neither via surface erosion nor via interparticle collisions due to the two following major reasons. First, Tb(III) lines are clearly absent when focusing near the ultrasonic horn at high distance from the surface (Figure 3). Second, molecular nitrogen or argon emission lines generally associated with triboluminescence (due to electric discharges with the intervening gas and solvent vapors)^{16–19} are not observed in our spectra, thus excluding this mechanism.

In addition, the experiments conducted with similar conditions using silica glass ($\text{Na}_2\text{O} \sim 15$ wt %, checked by EDX) and fused silica glass samples did not reveal any emission line, except the SL spectra resulting from the sonication of pure water. Note here that Na can be effectively excited with power ultrasound via collisional excitation mechanism.⁴ Fused silica is known to exhibit triboluminescence at 450 and 630 nm.²⁸ The absence of such kind of emission in our experiments even at short horn–sample distance indicates that the cavitation surface erosion has a negligible effect on the sonoexcitation of luminescent species. SEM and optical microscopy analyses were performed on the treated $(\text{Ce}_{0.9}\text{Tb}_{0.1})\text{PO}_4$ surfaces after sonolysis (see Figure S3, Supporting Information). While the short-distance treated samples exhibited damages due to cavitation erosion, the ~ 1 cm distance treated samples did not show any measurable damage at the surface. After several hours of ultrasonic treatment, only few imperfections can be seen due to the initial sintering and polishing of the surface. These observations are in

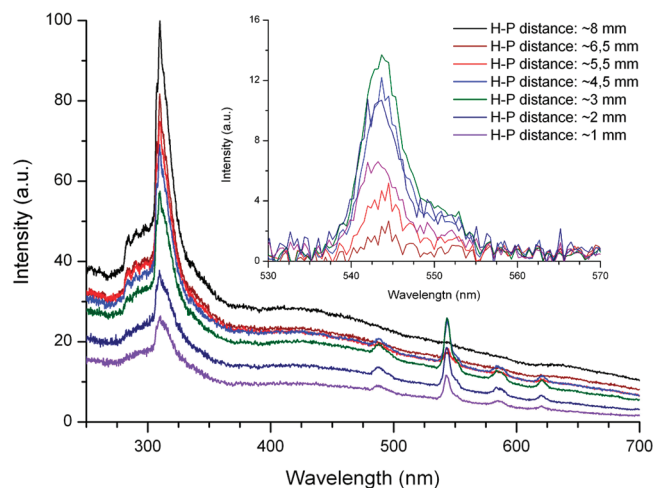


Figure 4. Evolution of the SL spectra (measured near the horn) as a function of the horn–pellet (H–P) distance (9 ± 1 °C, Ar, $I: \sim 18 \text{ W cm}^{-2}$). The values indicated in the caption indicate a stepwise decreasing distance between the horn and the sample. Inset: zoom of the 530 – 570 nm region corrected for the underlying continuum.

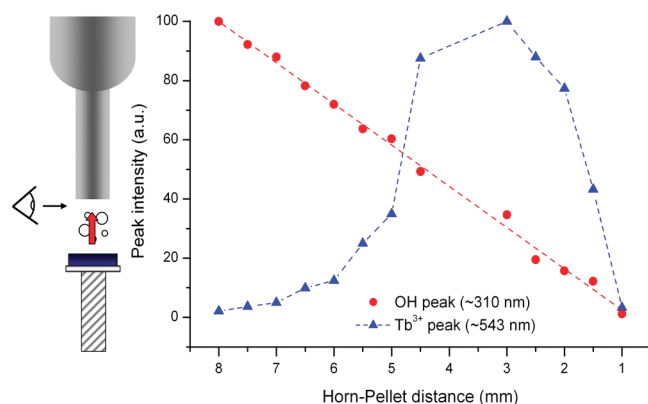


Figure 5. Normalized intensities observed for Tb(III) (~ 543 nm) and OH^* (~ 310 nm) main emission peaks (measured near the horn) as a function of the distance between the horn and the pellet.

agreement with previous investigations where acoustic cavitation damages were shown to be highly dependent upon the applied acoustic intensity and the horn–sample distance (cavitation erosion decreases dramatically with the distance).²³ It can thus be concluded that the sonoluminescence of Tb(III) does not originate from the $(\text{Ce}_{0.9}\text{Tb}_{0.1})\text{PO}_4$ matrix surface erosion.

To pursue the investigation of the excitation mechanism, the line intensities were compared as a function of the decreasing distance between the horn and the sample (Figure 4). Keeping the focus near the ultrasonic tip, where the emission intensity of excited OH^* radicals (OH^*) is maximal, the $(\text{Ce}_{0.9}\text{Tb}_{0.1})\text{PO}_4$ sample was approached from an initial distance of ~ 1 cm toward the sonotrode by using the Teflon screw situated under the reactor (Figure 1). As shown in Figure 5, the intensity of $\text{OH}(A^2\Sigma^+ - X^2\Pi)$ lines decreases almost linearly with the reducing distance, indicating a lower concentration of OH^* at the focusing point. This phenomenon most likely results from a shrinking of the cavitation zone due to the approaching solid sample. By contrast, Tb(III) emission lines initially observed at 488 , 543 , 584 , and 620 nm are totally absent when the solid surface is ~ 1 cm away; they slowly appear and

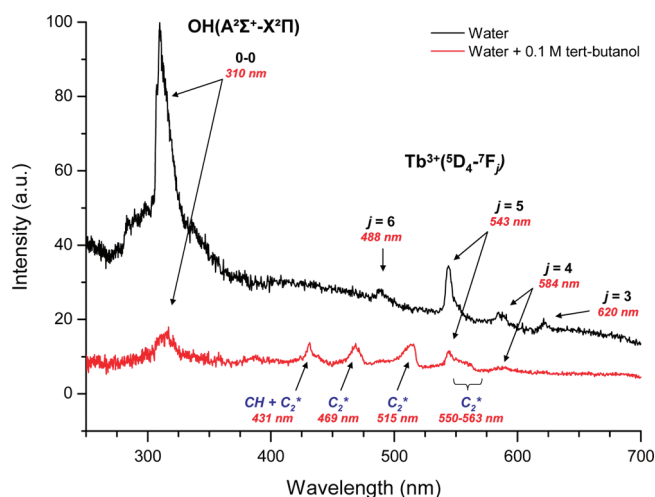


Figure 6. SL spectra measured for the sonication of $(\text{Ce}_{0.9}\text{Tb}_{0.1})\text{PO}_4$ pellet with optimized settings (short horn—sample distance, focusing near the ultrasonic horn, Ar, 9 ± 1 °C, $I: \sim 18 \text{ W cm}^{-2}$) in water (black curve) and after addition of 0.1 M *tert*-butanol (red curve).

increase when approaching the emitting solid surface (Figure 5). After having reached a maximum, Tb(III) intensity decreases jointly with both the SL continuum and the OH^* lines. Such a behavior fits well with the hypothesis in which the SL of Tb(III) is resulting from a re-emission of the water glow absorbed by the solid sample or, in other words, sonophotoluminescence. The intensity of Tb(III) SL as a function of the distance from the focusing point follows an inverse square relationship. Therefore, the observed SL intensity of Tb(III) sharply increases with the decrease of the distance in spite of the linear decrease of water SL intensity. However, at very short distance (around 1–3 mm) the intensity of the light source originated from water SL becomes insignificant, and the SL of Tb(III) is also strongly diminished. It is noteworthy that the surface erosion of $(\text{Ce}_{0.9}\text{Tb}_{0.1})\text{PO}_4$ pellet is clearly observed at such horn—surface distance (Figure S3 of Supporting Information), indicating the presence of strong acoustic cavitation when using these conditions.

The correlation between the intensities of water SL and Tb(III) emission line intensities was then investigated. We studied the SL in the presence of air and *tert*-butanol both known as quenchers of the SL while preserving cavitation and related sonochemical activity.^{9,29–31} Bubbling of air into the sonicated water presaturated with argon results in a dramatic decrease of SL including OH^* and Tb(III) lines (Figure S4, Supporting Information). Once argon is totally replaced with air, the SL is no more observable. Although SL disappears in the presence of air, acoustic cavitation at the surface is known to still occur.²³ Hence, this experiment supports the idea that Tb(III) emission is induced by sonoluminescence. When compared with the sonication of the pellet in argon saturated water, the addition of 0.1 M *tert*-butanol decreases dramatically the SL intensity (Figure 6). In addition, OH^* emission, as well as Tb(III) lines, almost completely vanishes. By contrast, new particular features appear and stand at 431, 469, 515, and 550–563 nm. These lines are attributed to the transitions $\text{d}^3\Pi_g - \text{a}^3\Pi_u$ of the excited C_2^* molecules, also called Swan bands.^{32,33} The large and intense peak at 431 nm was assigned to a combination of $\Delta v = +2$ of the $\text{d}^3\Pi_g - \text{a}^3\Pi_u$ Swan transition and to the $\text{A}^2\Delta - \text{X}^2\Pi$ transition of CH (see the detailed spectrum in Figure S5, Supporting Information). Note here that similar Swan

bands were observed during sonolysis of neat silicone oil and long chain hydrocarbons as well as water/benzene and water/ CCl_4 mixtures.^{32–34} The formation of C_2^* species in the sonochemical reactions is attributed to the pyrolysis of organic molecules or to their reactions with OH^* radicals inside the cavitation bubbles. Even if the total SL is decreased, the presence of Swan bands emission in our system univocally indicates that acoustic cavitation still occur in the presence of *tert*-butanol. Since Tb(III) lines disappear while acoustic cavitation still operates, this experiment definitely confirms the sonophotoexcitation origin of Tb(III) emission.

4. CONCLUSIONS

In summary, we have shown that the light emitted by an acoustically driven cloud of cavitating bubbles in cooled water saturated with argon enables to excite Tb(III) contained in a $(\text{Ce}_{0.9}\text{Tb}_{0.1})\text{PO}_4$ solid extended matrix. The mechanism of excitation originates from the photons emitted by the collapsing bubbles rather than from the shock wave or the thermal effects accompanying acoustic cavitation. It is important to emphasize that the mechanism of Tb(III) sonophotoluminescence in a solid matrix seems to be quite different from what happens in homogeneous solutions where Tb(III) ultrasonic excitation was claimed to be triggered by collisions with “hot” particles generated during cavitation bubble collapse rather than by sonophotoluminescence.¹⁵ We expect this work to contribute to a better understanding of the cavitation bubbles interaction with solid surfaces. Solid-state sonoluminescence has an evident potential as an experimental tool to study the mechanisms influencing ultrasonic treatment of solid surfaces. Moreover, the results reported here provide evidence that the light emitted during acoustic cavitation could strongly contribute to sonocatalytic phenomenon observed during advanced oxidation processes in the presence of ultrasonic waves and semiconductor catalysts.³⁵

■ ASSOCIATED CONTENT

S Supporting Information. Experimental details, SEM pictures, additional emission spectra, and XRD patterns of $(\text{Ce}_{0.9}\text{Tb}_{0.1})\text{PO}_4$ solid samples. This material is available free of charge via the Internet <http://pubs.acs.org>.

■ AUTHOR INFORMATION

Corresponding Author

*Phone: +33(0)4 66 33 92 51. Fax: +33(0)4 66 79 76 11.
E-mail: serguei.nikitenko@cea.fr.

■ ACKNOWLEDGMENT

We are very thankful to Tony Chave, Nicolas Clavier, and Renaud Podor (ICSM Marcoule) for help in the experiments and useful discussions. Matthieu Virot thanks CNRS for financial support.

■ REFERENCES

- (1) Suslick, K. S.; Flannigan, D. J. *Annu. Rev. Phys. Chem.* **2008**, *59*, 659.
- (2) Leighton, T. G. *The Acoustic Bubble*; Academic Press: London, 1994.
- (3) Cravotto, G.; Cintas, P. *Chem. Soc. Rev.* **2006**, *35*, 180.

- (4) Suslick, K. S. Sonoluminescence and Sonochemistry. In *Encyclopedia of Physical Science and Technology*, 3rd ed.; Meyers, R. A., Ed.; Academic Press: San Diego, CA, 2001; p 363.
- (5) Ashokkumar, M.; Grieser, F. *ChemPhysChem* **2004**, *5*, 439.
- (6) Flannigan, D. J.; Suslick, K. S. *Nature* **2005**, *434*, 52.
- (7) Flannigan, D. J.; Suslick, K. S. *Nature Phys.* **2010**, *6*, 598.
- (8) Pflieger, R.; Brau, H.-P.; Nikitenko, S. I. *Chem.—Eur. J.* **2010**, *16*, 11801.
- (9) Ashokkumar, M.; Grieser, F. *Chem. Commun.* **1998**, *5*, 561.
- (10) Hatanaka, S.; Mitome, H.; Yasui, K.; Kozuka, T.; Hayashi, S. *J. Am. Chem. Soc.* **2002**, *124*, 10250.
- (11) Grieser, F.; Ashokkumar, M. *Adv. Colloid Interface Sci.* **2001**, *89–90*, 423.
- (12) Ashokkumar, M.; Grieser, F. *Ultrason. Sonochem.* **1999**, *6*, 1.
- (13) Ashokkumar, M.; Grieser, F. *J. Am. Chem. Soc.* **2000**, *122*, 12001.
- (14) Sharipov, G. L.; Gainetdinov, R. Kh.; Abdrakhmanov, A. M. *JETP Lett.* **2006**, *83*, 493.
- (15) Sharipov, G. L.; Gainetdinov, R. Kh.; Abdrakhmanov, A. M. *Russ. Chem. Bull.* **2003**, *52*, 1969.
- (16) Eddingsaas, N. C.; Suslick, K. S. *Nature* **2006**, *444*, 163.
- (17) Eddingsaas, N. C.; Suslick, K. S. *J. Am. Chem. Soc.* **2007**, *129*, 6718.
- (18) Eddingsaas, N. C.; Suslick, K. S. *Phys. Rev. Lett.* **2007**, *99*, 234301.1.
- (19) Sharipov, G. L.; Gainetdinov, R. Kh.; Tukhbatullin, A. A. *Tech. Phys. Lett.* **2009**, *35*, 452.
- (20) Li, F.; Wang, M.; Mi, C.; Yi, K.; Xu, S. *J. Alloys Compd.* **2009**, *486*, L37.
- (21) Lin, S.; Yuan, Y.; Wang, H.; Jia, R.; Yang, X.; Liu, S. *J. Mater. Sci.: Mater. Electron.* **2009**, *20*, 899.
- (22) Di, W.; Wang, X.; Ren, X. *Nanotechnology* **2010**, *21*, 075709.1.
- (23) Virost, M.; Chave, T.; Nikitenko, S. I.; Shchukin, D. G.; Zemb, T.; Mohwald, H. *J. Phys. Chem. C* **2010**, *114*, 13083.
- (24) Hagenson, L. C.; Doraiswamy, L. K. *Chem. Eng. Sci.* **1998**, *53*, 131.
- (25) You, H.; Wu, X.; Cui, H.; Hong, G. *J. Luminesc.* **2003**, *104*, 223.
- (26) Kijkowska, R. *J. Mater. Sci.* **2003**, *38*, 229.
- (27) Cetiner, Z. S.; Wood, S. A.; Gammons, C. H. *Chem. Geol.* **2005**, *217*, 147.
- (28) Miura, T.; Hosobuchi, E.; Arawaka, I. *Vacuum* **2010**, *84*, 573.
- (29) Young, F. R. *Sonoluminescence*; CRC Press: Boca Raton, FL, 2005; Chapter 2.
- (30) Arakeri, V. H. *Pramana J. Phys.* **1993**, *40*, L145.
- (31) Flannigan, D. J.; Suslick, K. S. *J. Phys. Chem. A* **2006**, *30*, 9315.
- (32) Flint, E. B.; Suslick, K. S. *J. Am. Chem. Soc.* **1989**, *111*, 6987.
- (33) Suslick, K. S.; Flint, E. B. *Nature* **1987**, *330*, 553.
- (34) Didenko, Yu. T.; McNamara, W. B., III; Suslick, K. S. *J. Phys. Chem. A* **1999**, *103*, 10783.
- (35) Adewuyi, Y. G. *Environ. Sci. Technol.* **2005**, *39*, 8557.